Wetting of a selective solid surface by an asymmetric binary mixture

Jörg R. Silbermann,* Dirk Woywod,† and Martin Schoen‡
Stranski-Laboratorium für Physikalische und Theoretische Chemie, Sekr. TC 7, Fakultät für Mathematik und Naturwissenschaften, Technische Universität Berlin, Straße des 17. Juni 124, D-10623 Berlin, Germany
(Received 23 October 2003; published 31 March 2004)

We consider a lattice-gas model of an asymmetric binary mixture in which the attraction between a pair of molecules of species *A* exceeds that between a pair of molecules of species *B*. The interaction between two molecules of species *A* and *B* is chosen to promote the formation of demixed *A*-rich liquid bulk phases. Molecules interact with a selective solid wall, preferentially adsorbing molecules of species *B*. Positions of molecules are restricted to sites on a simple-cubic lattice. We invoke a mean-field representation of the Hamiltonian governing all intermolecular interactions and assume only nearest-neighbor attractions. Minimizing the grand-potential functional of the lattice gas numerically, phase diagrams for films wetting the solid substrate are obtained. One of our key findings concerns *B*-rich mixed or demixed films forming in the vicinity of the solid surface and coexisting with demixed *A*-rich films. The formation of *B*-rich films can be understood as a result of the competition between the asymmetry of the (bulk) mixture and the selectivity of the solid surface. The concentration of component *B* in *B*-rich mixed films shows a peculiar temperature dependence. It first increases with temperature T until an ''inversion'' temperature T_{inv} is reached, and then declines for $T \geqslant T_{\mathrm{inv}}$ until the critical point between (demixed) *A*- and *B*-rich films is reached.

DOI: 10.1103/PhysRevE.69.031606 PACS number(s): 68.08.Bc, 05.70.Np, 61.46.+w, 68.55.Nq

I. INTRODUCTION

If a fluid interacts with a solid substrate a wealth of surface-induced phase transitions arises that are generally subsumed under the term ''wetting'' [1–5]. Wetting phenomena are of practical importance in a variety of contexts. They determine how paints stick to solid surfaces or how detergents remove stains from fabric [6]. Moreover, wetting is the key issue in an important emerging and rapidly developing field of technology known as ''nanofluidics,'' where wetting characteristics of nanostructured solid surfaces are utilized to manipulate tiny amounts of fluid [7–9].

Investigations of wetting phenomena at a molecular level have a long history [10]. One of the earliest attempts to classify systems with respect to their wetting behavior is a study by Dash, who analyzed experimental sorption isotherms of physisorbed gases [11]. It was subsequently realized that wetting phenomena may be perceived as substrate-induced phase transitions. An example are transitions from partial to complete wetting analyzed in the seminal papers by Cahn [12] and Ebner and Saam [13,14]. Later Pandit *et al.*, who built on Dash's study, presented a more comprehensive investigation of multilayer adsorption on attractive solid substrates [15]. Since then more specialized topics in the context of wetting have been considered. Examples include the nature of the prewetting critical point [16], the order of wetting transitions [17,18], or the wetting of structured surfaces [19–22].

Whereas the wetting of planar substrates (structured or not) by pure fluids is quite well understood, less work has been devoted to binary mixtures [5]. Theoretically, most studies are concerned with a rather simplistic model, namely, that of a *symmetric* binary mixture in which the interactions between like molecules of both components as well as their sizes are set equal [23–25]. For such a mixture Schmid and Wilding focus on the wetting of nonselective substrates, that is, a solid surface that does not prefer molecules of either component energetically [23]. For this system Wilding *et al.* have determined the bulk phase diagram in an earlier paper based on Monte Carlo and mean-field calculations [26]. A slightly more complex situation was considered by Fan *et al.* [24] and Kierlik *et al.* [25] who employed selective solid substrates in their work on wetting characteristics of symmetric binary mixtures.

However, with respect to experimental systems solid substrates should not only be selective for mixture components but the mixture itself should be asymmetric, that is, the interaction between like molecules of one species should differ from that between molecules of the other mixture component. Even though this situation is the experimentally most relevant one, little theoretical attention has been given to it thus far. An exception (and to the best of our knowledge the only one) is the work by Choudhury and Ghosh, who consider an asymmetric binary mixture of Lennard-Jones molecules in slit pores [27]. However, these authors are interested in confinement effects rather than wetting phenomena occurring at a *single* solid surface which are the focal point of the present study.

Since the dimension of the parameter space necessary to describe an asymmetric binary mixture at a selective solid surface is already quite large, we base our work on a lattice model in which positions of molecules are restricted to sites of a simple-cubic lattice. We simplify our model even further by considering only short-range (i.e., nearest-neighbor) interactions among molecules. Thus, we implicitly limit our work to (complete) wetting excluding, to some extent, phenomena like, say, prewetting which occurs only in the presence of

*Electronic address: joerg.silbermann@fluids.tu-berlin.de
†Electronic address: dirk.woywod@fluids.tu-berlin.de
‡Electronic address: martin.schoen@fluids.tu-berlin.de

long-range surface interactions [28]. Within a mean-field approximation for the intrinsic free-energy functional, we employ density functional theory to determine the phase behavior of this model [29].

The model has been successfully employed in the past to investigate confinement-driven phase transitions in nanoporous media where, however, the emphasis was strictly on *symmetric* binary mixtures and the pore walls are nonselective [29]. The bulk behavior of such a symmetric binary lattice gas is qualitatively similar to the one observed earlier by Wilding *et al.* for their related but continuous symmetric model mixture [26]. Wetting of an isolated solid surface has also been studied for this model [30].

In the present paper we extend the model of Woywod and Schoen [29,30] to the case of asymmetric binary mixtures wetting a selective, planar, and a chemically homogeneous substrate surface. Our paper is organized as follows. In Sec. II we outline the theoretical foundations of our study where we introduce the model in Sec. II A and develop its mean-field theoretical treatment in Sec. II B. Section III is given to a consideration of thermodynamic equilibrium states. We begin in Sec. III A with a brief discussion of the limit of vanishing temperature in which we can solve our model analytically. The more general case of nonvanishing temperatures is considered in Sec. III B, where symmetry considerations are employed in Sec. III C to reduce the numerical burden. The determination of phase diagrams is outlined in Sec. III D. Section IV is devoted to a presentation of our results starting with the bulk in Sec. IV A and continuing with wetting phenomena in Sec. IV B. Finally, we summarize our findings in Sec. V.

II. THEORY

A. Model system

We consider a binary (A-B) mixture on a simple cubic lattice of $\mathcal{N}=nz$ sites, whose lattice constant is ℓ. The position of a fluid molecule on this lattice is specified by a pair of integers (k,l) where $1\leqslant k\leqslant n$ labels the position in an x-y plane and $1\leqslant l\leqslant z$ determines the position of that plane along the z axis. A specific site may be occupied either by a molecule of species A or B, or it may be altogether empty. To describe individual configurations on the lattice we introduce a matrix $\mathbf{s}$ of occupation numbers such that

$$s_{k,l}=\begin{cases}+1, & \text{site occupied by molecule of component } A\\ 0, & \text{empty site}\\ -1, & \text{site occupied by molecule of component } B.\end{cases} \tag{2.1}$$

For a given configuration $\mathbf{s}$ the total number of sites occupied by molecules of species A or B is given by $N_A(\mathbf{s})$ or $N_B(\mathbf{s})$, respectively, for which explicit expressions are given in Eqs. (2.2a) and (2.2b) in the paper by Woywod and Schoen [29]. Based upon these expressions Woywod and Schoen also calculated the total number of A-$A[N_{AA}(\mathbf{s})]$, B-$B[N_{BB}(\mathbf{s})]$, and A-B nearest-neighbor pairs $[N_{AB}(\mathbf{s})]$ on the lattice [see Eqs. (2.6a), (2.6b), and (2.6c) in Ref. [29]]. We *formally* confine the mixture by two impenetrable solid substrates located at $l=0$ and $l=z+1$ and introduce the number of molecules of type A at those substrates, $N_{AW}(\mathbf{s})$, and that of type B, $N_{BW}(\mathbf{s})$, respectively [see Eqs. (2.4) and (2.5) of Ref. [29]].

In addition, we assume all interactions to be pairwise additive and model them according to square-well potentials where the width of the attractive well is set equal to the diameter σ of a fluid molecule (taking the same value of σ for both species). Hence, we restrict ourselves exclusively to nearest-neighbor attractions. The assumption of a maximum occupation of each site by at most one molecule [see Eq. (2.1)] accounts for the infinitely hard core imposed by the square-well potential.

The energy function (i.e., the Hamiltonian) governing our system can then be cast as

$$\begin{aligned}\mathcal{H}(\mathbf{s})=&\epsilon[N_{AA}(\mathbf{s})+\chi_B N_{BB}(\mathbf{s})]+\epsilon_{AB}N_{AB}(\mathbf{s})\\&+\epsilon_W[N_{AW}(\mathbf{s})+\chi_W N_{BW}(\mathbf{s})]-\mu[N_A(\mathbf{s})+N_B(\mathbf{s})],\end{aligned} \tag{2.2}$$

where

$$\epsilon\equiv\epsilon_{AA}, \tag{2.3a}$$

$$\epsilon_W\equiv\epsilon_{AW}, \tag{2.3b}$$

$$\chi_B\equiv\frac{\epsilon_{BB}}{\epsilon_{AA}}, \tag{2.3c}$$

$$\chi_W\equiv\frac{\epsilon_{BW}}{\epsilon_{AW}}. \tag{2.3d}$$

In Eqs. (2.3), ϵ determines the depth of the attractive well (i.e., the attraction strength) of the A-A potential function. Likewise, ϵ_W describes the attraction of a molecule of species A by the solid substrate.

Parameter χ_B will henceforth be referred to as the ''asymmetry'' of the model mixture where $\chi_B>1$ characterizes a binary mixture in which the formation of B-B pairs is energetically favored whereas for $\chi_B<1$ this is the case for A-A pairs. For the special case $\chi_B=1$ the asymmetric mixture degenerates to the symmetric case previously studied in Refs. [29,30]. In addition, we define the ''selectivity'' of the solid surfaces by specifying χ_W in Eq. (2.3d) in a fashion similar to χ_B in Eq. (2.3c). Hence, the parameter space of our model is spanned by the set $\{\epsilon,\epsilon_{AB},\epsilon_W,\chi_B,\chi_W\}$. To limit the complexity of our model we deliberately choose

$$\mu\equiv\mu_A=\mu_B \tag{2.4}$$

in all the calculations of this work [see Eq. (2.2)].

Based upon these considerations we may readily introduce the partition function in the grand canonical ensemble via [31]

$$\Xi(\mathcal{N},T,\mu)=\sum_{\{\mathbf{s}\}}\exp[-\beta\mathcal{H}(\mathbf{s})]\equiv\exp(-\beta\Omega), \tag{2.5}$$

where $\Omega(\mathcal{N},T,\mu)$ is the grand potential and $\mathcal{N}$ is the "volume" (i.e., the number of sites) on the lattice.

B. Mean-field treatment

To proceed we introduce a mean-field approximation for the Hamiltonian specified in Eq. (2.2). It consists of *assuming* that within each plane l parallel to the solid substrates the occupation number at each lattice site can be replaced by an *average* occupation number for the entire plane. On account of the symmetry-breaking nature of the solid substrate these average occupation numbers will generally vary between planes, that is they will change with l. Hence, we introduce the total *local* density,

$$\rho_l=\rho_l^A+\rho_l^B=\frac{1}{n}\sum_{k=1}^{n} s_{k,l}^2\equiv\frac{n_l^A+n_l^B}{n}\equiv\frac{n_l}{n}, \tag{2.6}$$

and the *local* "miscibility" m_l,

$$m_l\rho_l=\rho_l^A-\rho_l^B=\frac{1}{n}\sum_{k=1}^{n} s_{k,l}, \tag{2.7}$$

as convenient alternative order parameters at the mean-field level. In the thermodynamic limit $n\to\infty$, ρ_l (in units of ℓ^3) is dimensionless and continuous on the interval $[0,1]$ which implies that m_l is continuous and dimensionless as well but on the interval $[-1,1]$.

Mathematically speaking, the mean-field assumption consists of mapping the $n\times z$ occupation-number matrix $\mathbf{s}$ onto the z-dimensional vectors $\boldsymbol{n}^A=(n_1^A,n_2^A,\ldots,n_z^A)$ and $\boldsymbol{n}^B=(n_1^B,n_2^B,\ldots,n_z^B)$ where n_l^i is the *total* number of molecules of species i on lattice plane l *regardless* of their specific arrangement. Hence, we replace $H(\boldsymbol{s})$ by its mean-field analog $H_{mf}(\boldsymbol{n}^A,\boldsymbol{n}^B)$, where we note in passing that the transformation $\mathbf{s}\to\boldsymbol{n}^A,\boldsymbol{n}^B$ is not bijective in general (also see Sec. III A).

To derive the mean-field analog of Eq. (2.5) we rewrite it more explicitly as

$$\begin{aligned}\Xi&=\sum_{s_{1,1}=-1}^{1}\sum_{s_{2,1}=-1}^{1}\cdots\sum_{s_{n,z}=-1}^{1}\exp[-\beta\mathcal{H}(\mathbf{s})]\\&=\left(\prod_{l=1}^{z}\sum_{s_{1,l}=-1}^{1}\sum_{s_{2,l}=-1}^{1}\cdots\sum_{s_{n,l}=-1}^{1}\right)\exp[-\beta\mathcal{H}(\mathbf{s})].\end{aligned} \tag{2.8}$$

Hence, at the mean-field level, we may replace the $n\times z$ sums in parentheses above according to

$$\begin{aligned}\Xi\to\Xi_{mf}=&\left(\prod_{l=1}^{z}\sum_{n_l^A=0}^{n}\sum_{n_l^B=0}^{n-n_l^A}\right)\Theta(\boldsymbol{n}^A,\boldsymbol{n}^B)\\&\times\exp[-\beta\mathcal{H}_{mf}(\boldsymbol{n}^A,\boldsymbol{n}^B)],\end{aligned} \tag{2.9}$$

where the combinatorial factor

$$\Theta(\boldsymbol{n}^A,\boldsymbol{n}^B)=\prod_{l=1}^{z}\binom{n}{n_l^A+n_l^B}\binom{n_l^A+n_l^B}{n_l^A}=\prod_{l=1}^{z}\binom{n}{n_l}\binom{n_l}{n_l^A} \tag{2.10}$$

represents the *a priori* possible configurations corresponding to the same value of $\mathcal{H}_{mf}$, that is, the degeneracy of a particular microstate characterized by vectors $\boldsymbol{n}^A$ and $\boldsymbol{n}^B$.

In the thermodynamic limit (i.e., as $n\to\infty$) it is convenient to replace the discrete variables n_l^i by their (quasi–) continuous counterparts $\rho_l^i=n_l^i/n$ so that the double sums can be replaced by double integrals, that is,

$$\sum_{n_l^A=0}^{n}\sum_{n_l^B=0}^{n-n_l^A}\cdots\overset{n\gg1}{\to}n^2\int_0^1 d\rho_l^A\int_0^{1-\rho_l^A}d\rho_l^B\ldots,$$

where the z-dimensional vectors $\boldsymbol{\rho}^A$ and $\boldsymbol{\rho}^B$ are defined analogously to $\boldsymbol{n}^A$ and $\boldsymbol{n}^B$, respectively. Changing variables $\rho_l^A,\rho_l^B\to\rho_l,m_l$ via Eqs. (2.6) and (2.7) in this last expression permits us to eventually cast Eq. (2.9) as

$$\begin{aligned}\Xi_{mf}&=n^{2z}\left(\prod_{l=1}^{z}\int_0^1 d\rho_l^A\int_0^{1-\rho_l^A}d\rho_l^B\right)\Theta(\boldsymbol{\rho}^A,\boldsymbol{\rho}^B)\\&\quad\times\exp[-\beta\mathcal{H}_{mf}(\boldsymbol{\rho}^A,\boldsymbol{\rho}^B;\mu)]\\&=\frac{n^{2z}}{2^z}\int\boldsymbol{\rho}\;d\boldsymbol{\rho}\int d\boldsymbol{m}\Theta(\boldsymbol{\rho},\boldsymbol{m})\\&\quad\times\exp[-\beta\mathcal{H}_{mf}(\boldsymbol{\rho},\boldsymbol{m};\mu)]\\&\equiv\frac{n^{2z}}{2^z}\int\boldsymbol{\rho}\;d\boldsymbol{\rho}\int d\boldsymbol{m}\exp\\&\quad\times[-\beta\omega(\boldsymbol{\rho},\boldsymbol{m};T,\mu)],\end{aligned} \tag{2.11}$$

where $\omega(\boldsymbol{\rho},\boldsymbol{m};T,\mu)$ defines an energy hyperplane in the multidimensional space spanned by the set of local order parameters $\{\boldsymbol{\rho},\boldsymbol{m}\}$ for given values of T and μ.

The function $\omega(\boldsymbol{\rho},\boldsymbol{m};T,\mu)$ may have many extrema in $\boldsymbol{\rho}$–$\boldsymbol{m}$ space. The necessary conditions for these extrema to exist may be stated as

$$\frac{\partial\omega(\boldsymbol{\rho},\boldsymbol{m};T,\mu)}{\partial\rho_k}=h_1^k(\rho_{k-1},m_{k-1},\rho_k,m_k,\rho_{k+1},m_{k+1})=0, \tag{2.12a}$$

$$\frac{\partial\omega(\boldsymbol{\rho},\boldsymbol{m};T,\mu)}{\partial m_k}=h_2^k(\rho_{k-1},m_{k-1},\rho_k,m_k,\rho_{k+1},m_{k+1})=0, \tag{2.12b}$$

where explicit expressions for the functions h_1^k and h_2^k are given in Eqs. (B5). Equations (2.12) may have several solutions $\alpha=1,\ldots,i$. It is then sensible to introduce the notion of a phase $\mathcal{P}^\alpha$ through the set of $2z$ elements

$$\mathcal{P}^\alpha=\{\boldsymbol{\rho}^\alpha,\boldsymbol{m}^\alpha\} \tag{2.13}$$

where $\boldsymbol{\rho}^{\alpha}$ and $\boldsymbol{m}^{\alpha}$ are not only simultaneous solutions of Eqs. (2.12) but also *minima* of $\omega(\boldsymbol{\rho},\boldsymbol{m};T,\mu)$. At this point it is important to realize that in the thermodynamic limit (i.e., as $n\to\infty$) the global minimum $\boldsymbol{\rho}^*$, $\boldsymbol{m}^*$ of the function ω will completely determine the integral in Eq. (2.11). In the limit $n\to\infty$, this permits us to rewrite Eq. (2.11) as

$$\begin{aligned}\omega(T,\mu)&=\frac{\Omega_{mf}}{\mathcal{N}}\\&=-\frac{\ln\Xi_{mf}(\mathcal{N},T,\mu)}{\beta\mathcal{N}}\\&=-\frac{\ln\Theta(\boldsymbol{\rho}^*,\boldsymbol{m}^*)}{\beta\mathcal{N}}+\frac{\mathcal{H}_{mf}(\boldsymbol{\rho}^*,\boldsymbol{m}^*)}{\mathcal{N}}\end{aligned}\tag{2.14}$$

where $\boldsymbol{\rho}^*$ and $\boldsymbol{m}^*$ represent the ''configuration'' at the absolute minimum of the grand–potential density $\omega(T,\mu)$, that is the thermodynamically stable phase $\mathcal{P}^*$ whereas all other $i-1$ phases are only metastable (except for points of phase coexistence, see Sec. III D).

III. EQUILIBRIUM STATES

A. Limit of vanishing temperature

Let us now briefly discuss the special case in which the transformation $s_{k,l}\to\rho_l,m_l$ is bijective. From the definition of ρ_l and m_l in Eqs. (2.6) and (2.7) it is immediately clear that this can only be the case if all matrix elements in the mth row of **s** are equal assuming one of the three values given in Eq. (2.1). This then implies that $\rho_l=0,1$ is discrete and double–valued. In other words, across any given lattice plane l *all* sites must be empty, or occupied by molecules of one or the other species so that $\rho_l=\rho_l^A=1$ or $\rho_l=\rho_l^B=1$, respectively. To discriminate between these cases, Eq. (2.7) gives $m_l=1$ if $\rho_l=\rho_l^A=1$ whereas $m_l=-1$ if $\rho_l=\rho_l^B=1$. Thus,

$$n_l=n,\tag{3.1a}$$

$$n_l^A=\begin{cases}0\\n_l,\end{cases}\tag{3.1b}$$

implying $\Theta=1$ from Eq. (2.10), which is mathematically equivalent to saying that the transformation $s_{k,l}\to\rho_l,m_l$ is bijective.

If this is so we conclude from Eq. (2.11) that

$$\omega^{\alpha}(\mathcal{P}^{\alpha};T,\mu)=\frac{\mathcal{H}_{mf}(\mathcal{P}^{\alpha})}{\mathcal{N}}.\tag{3.2}$$

This latter expression is identical to Eq. (2.14) in the limit $T=0$ replacing, however, in Eq. (3.2), $\mathcal{P}^{\alpha}$ by $\mathcal{P}^*$. Thus, in this sense

$$\omega_0(\mu)=\omega_0(\mathcal{P}^*;\mu)=\frac{\mathcal{H}_{mf}(\mathcal{P}^*)}{\mathcal{N}}\tag{3.3}$$

is a consequence of the fact that at $T=0$ the mean-field treatment becomes exact (i.e., the transformation $s_{k,l}\to\rho_l,m_l$ becomes bijective) where the subscript ''0'' was introduced to emphasize the limit $T=0$. Equation (3.2) is important because $\mathcal{H}_{mf}(\mathcal{P}^{\alpha})$ can be calculated analytically for our present model [32].

B. Nonvanishing temperatures

For $T>0$ we are concerned with solutions of Eqs. (2.12). To find these it is convenient to introduce the (transpose of the) $2z$-dimensional vector

$$\boldsymbol{x}^{\mathrm{T}}=(\rho_1,m_1,\ldots,\rho_l,m_l,\ldots,\rho_z,m_z)\tag{3.4}$$

which permits us to rewrite Eqs. (2.12) as

$$\boldsymbol{f}(\boldsymbol{x})=\begin{pmatrix}h_1^1(\rho_0,m_0,\rho_1,m_1,\rho_2,m_2)\\h_2^1(\rho_0,m_0,\rho_1,m_1,\rho_2,m_2)\\\vdots\\h_1^l(\rho_{l-1},m_{l-1},\rho_l,m_l,\rho_{l+1},m_{l+1})\\h_2^l(\rho_{l-1},m_{l-1},\rho_l,m_l,\rho_{l+1},m_{l+1})\\\vdots\\h_1^z(\rho_{z-1},m_{z-1},\rho_z,m_z,\rho_{z+1},m_{z+1})\\h_2^z(\rho_{z-1},m_{z-1},\rho_z,m_z,\rho_{z+1},m_{z+1})\end{pmatrix}\overset{!}{=}\mathbf{0}.\tag{3.5}$$

Suppose a solution $\boldsymbol{x}_0$ of Eq. (3.5) exists for a given temperature T_0 and a chemical potential μ_0. We are then seeking a solution $\boldsymbol{x}$ for slightly different thermodynamic conditions

$$T=T_0+\delta T,\tag{3.6a}$$

$$\mu=\mu_0+\delta\mu,\tag{3.6b}$$

where δT and $\delta\mu$ are sufficiently small so that we may expand Eq. (3.5) in a Taylor series around $\boldsymbol{x}_0$,

$$\boldsymbol{f}(\boldsymbol{x})=\boldsymbol{f}(\boldsymbol{x}_0)+\boldsymbol{\nabla}\boldsymbol{f}^{\mathrm{T}}(\boldsymbol{x})\big|_{\boldsymbol{x}=\boldsymbol{x}_0}\cdot(\boldsymbol{x}-\boldsymbol{x}_0)+\mathcal{O}(|\boldsymbol{x}-\boldsymbol{x}_0|^2)\equiv\mathbf{0},\tag{3.7}$$

retaining only the linear term where the z-dimensional vector $\boldsymbol{\nabla}^{\mathrm{T}}=(\partial/\partial\rho_1,\partial/\partial m_1,\ldots,\partial/\partial\rho_z,\partial/\partial m_z)$. Introducing the functional matrix $\mathbf{D}$ through the dyad $\boldsymbol{\nabla}\boldsymbol{f}^{\mathrm{T}}(\boldsymbol{x})$, that is

$$\mathbf{D}\equiv\boldsymbol{\nabla}\boldsymbol{f}^{\mathrm{T}}(\boldsymbol{x})=\begin{pmatrix}\frac{\partial h_1^1}{\partial\rho_1}&\frac{\partial h_2^1}{\partial\rho_1}&\cdots&\frac{\partial h_2^z}{\partial\rho_1}\\\frac{\partial h_1^1}{\partial m_1}&\frac{\partial h_2^1}{\partial m_1}&\cdots&\frac{\partial h_2^z}{\partial m_1}\\\vdots&\vdots&\ddots&\vdots\\\frac{\partial h_1^1}{\partial\rho_z}&\frac{\partial h_2^1}{\partial\rho_z}&\cdots&\frac{\partial h_2^z}{\partial\rho_z}\\\frac{\partial h_1^1}{\partial m_z}&\frac{\partial h_2^1}{\partial m_z}&\cdots&\frac{\partial h_2^z}{\partial m_z}\end{pmatrix},\tag{3.8}$$

we can solve Eq. (3.7) iteratively by rewriting it as

$$\boldsymbol{x}_{i+1} = -\mathbf{D}^{-1}\cdot\boldsymbol{f}(\boldsymbol{x}_i) + \boldsymbol{x}_i \equiv \delta\boldsymbol{x}_i + \boldsymbol{x}_i \tag{3.9}$$

where Eq. (3.5) has also been used and the elements of **D** can easily be computed with the aid of Eqs. (B5).

C. Symmetry considerations

Since we restrict ourselves to nearest-neighbor interactions, $h_{1,2}^k$ depend only on the set of variables $\{\rho_j, m_j | k-1 \leqslant j \leqslant k+1\}$ as one can verify from Eqs. (B5). Hence, **D** in Eq. (3.8) has a band structure where all elements

$$\frac{\partial h_{1,2}^i}{\partial \rho_j} = 0, \tag{3.10a}$$

$$\frac{\partial h_{1,2}^i}{\partial m_j} = 0, \quad \forall |i-j| \geqslant 2. \tag{3.10b}$$

Moreover, since $\omega(\mathcal{P})$ is continuous and differentiable we have

$$\frac{\partial h_1^k}{\partial m_l} = \frac{\partial^2 \omega}{\partial m_l \partial \rho_k} = \frac{\partial^2 \omega}{\partial \rho_k \partial m_l} = \frac{\partial h_2^k}{\partial \rho_k}, \quad \forall k,l; \tag{3.11}$$

that is **D** is symmetric with respect to its main diagonal. Since in this work we focus on planar, chemically homogeneous substrates an additional symmetry exists for the local order parameters with respect to a (virtual) midplane on the lattice which may coincide with an actual lattice plane if z is odd. Therefore, if z is odd we conclude that

$$\rho_{\Phi-k} = \rho_{\Phi+k}, \tag{3.12a}$$

$$m_{\Phi-k} = m_{\Phi+k}, \quad k = 1, \ldots, \Phi-1, \tag{3.12b}$$

where $\Phi = (z+1)/2$. If, on the other hand, z is even,

$$\rho_{\Phi-k+1} = \rho_{\Phi+k}, \tag{3.13a}$$

$$m_{\Phi-k+1} = m_{\Phi+k}, \quad k = 1, \ldots, \Phi, \tag{3.13b}$$

where now, of course, $\Phi = z/2$.

To simplify the subsequent discussion we restrict ourselves to the case of even z where we note in passing that for sufficiently large z the distinction between odd and even numbers of lattice planes becomes, of course, irrelevant. Then we may reorganize the $2z$ elements of vectors $\boldsymbol{x}$, $\boldsymbol{f}$, and $\boldsymbol{\nabla}$ such that the resulting matrix **D** has point symmetry with respect to an inversion center. More specifically, we may express **D** formally as

$$\mathbf{D} = \begin{pmatrix} \tilde{\mathbf{A}} & \tilde{\mathbf{B}} \\ \mathbf{B} & \mathbf{A} \end{pmatrix}, \tag{3.14}$$

where elements of the submatrices are related through

$$\tilde{A}_{\Phi-k+1,\Phi-l+1} = A_{k,l} \tag{3.15a}$$

$$\tilde{B}_{\Phi-k+1,\Phi-l+1} = B_{k,l}, \quad k,l = 1, \ldots, z. \tag{3.15b}$$

It is then easy to verify that

$$\tilde{\mathbf{B}} = \begin{pmatrix} 0 & & \cdots & & 0 \\ \vdots & \ddots & & & \vdots \\ \dfrac{\partial h_2^{\Phi+1}}{\partial \rho_\Phi} & \dfrac{\partial h_1^{\Phi+1}}{\partial \rho_\Phi} & 0 & \cdots & 0 \\ \dfrac{\partial h_2^{\Phi+1}}{\partial m_\Phi} & \dfrac{\partial h_1^{\Phi+1}}{\partial m_\Phi} & 0 & \cdots & 0 \end{pmatrix}, \tag{3.16}$$

that is, it contains only four nonzero elements. Similarly, the last two rows of submatrix $\tilde{\mathbf{A}}$ can be cast as

$$\tilde{\mathbf{A}} = \begin{pmatrix} \vdots & & & \cdots & & & \\ 0 & \cdots & 0 & \dfrac{\partial h_1^{\Phi-1}}{\partial \rho_\Phi} & \dfrac{\partial h_2^{\Phi-1}}{\partial \rho_\Phi} & \dfrac{\partial h_1^{\Phi}}{\partial \rho_\Phi} & \dfrac{\partial h_2^{\Phi}}{\partial \rho_\Phi} \\ 0 & \cdots & 0 & \dfrac{\partial h_2^{\Phi-1}}{\partial m_\Phi} & \dfrac{\partial h_1^{\Phi-1}}{\partial m_\Phi} & \dfrac{\partial h_2^{\Phi}}{\partial m_\Phi} & \dfrac{\partial h_1^{\Phi}}{\partial m_\Phi} \end{pmatrix}. \tag{3.17}$$

One then realizes that in $\tilde{\mathbf{A}}$ the element

$$\frac{\partial h_2^{\Phi}}{\partial \rho_\Phi} = \frac{\partial^2 \omega}{\partial \rho_\Phi \partial m_\Phi} = \frac{\partial^2 \omega}{\partial m_\Phi \partial \rho_\Phi} \tag{3.18}$$

appears, whereas in $\tilde{\mathbf{B}}$ the conjugate element

$$\frac{\partial h_2^{\Phi+1}}{\partial \rho_\Phi} = \frac{\partial^2 \omega}{\partial \rho_\Phi \partial m_{\Phi+1}} = \frac{\partial^2 \omega}{\partial m_{\Phi+1} \partial \rho_\Phi} \tag{3.19}$$

arises. Similar considerations apply to the pair of elements $\partial h_1^{\Phi}/\partial \rho_\Phi$ and $\partial h_1^{\Phi+1}/\partial \rho_\Phi$ as well as to the corresponding two pairs of elements on the last rows of $\tilde{\mathbf{A}}$ and $\tilde{\mathbf{B}}$. Moreover, it is apparent from symmetry properties stated in Eqs. (3.13) (z even) that both $\partial h_2^{\Phi}/\partial \rho_\Phi$ and $\partial h_2^{\Phi+1}/\partial \rho_\Phi$ are acting on the same element of the vector $\boldsymbol{x} - \boldsymbol{x}_0$ in Eq. (3.7) such that Eq. (3.14) can be recast as

$$\mathbf{D}' = \begin{pmatrix} \tilde{\mathbf{A}}' & \mathbf{0} \\ \mathbf{0} & \mathbf{A}' \end{pmatrix} \tag{3.20}$$

where **0** is the $z \times z$ zero matrix, $\tilde{\mathbf{A}}'$ is identical with $\tilde{\mathbf{A}}$ except for the last two elements in the two bottom rows, that is [see Eq. (3.17)],

$$\tilde{\mathbf{A}}' = \begin{pmatrix} \vdots & & & \cdots & & & & \\ 0 & \cdots & 0 & \dfrac{\partial h_1^{\Phi-1}}{\partial \rho_\Phi} & \dfrac{\partial h_2^{\Phi-1}}{\partial \rho_\Phi} & \left(\dfrac{\partial h_1^{\Phi}}{\partial \rho_\Phi}+\dfrac{\partial h_1^{\Phi}}{\partial \rho_{\Phi+1}}\right) & \left(\dfrac{\partial h_1^{\Phi}}{\partial m_\Phi}+\dfrac{\partial h_1^{\Phi}}{\partial m_{\Phi+1}}\right) \\ 0 & \cdots & 0 & \dfrac{\partial h_2^{\Phi-1}}{\partial m_\Phi} & \dfrac{\partial h_1^{\Phi-1}}{\partial m_\Phi} & \left(\dfrac{\partial h_2^{\Phi}}{\partial \rho_\Phi}+\dfrac{\partial h_2^{\Phi}}{\partial \rho_{\Phi+1}}\right) & \left(\dfrac{\partial h_2^{\Phi}}{\partial m_\Phi}+\dfrac{\partial h_2^{\Phi}}{\partial m_{\Phi+1}}\right) \end{pmatrix}, \tag{3.21}$$

and the relation between the new submatrices $\tilde{\mathbf{A}}'$ and $\mathbf{A}'$ is the same as that between $\tilde{\mathbf{A}}$ and $\mathbf{A}$ [see Eq. (3.15a)].

Because of these symmetry considerations we may replace Eq. (3.9) by

$$\tilde{\boldsymbol{x}}_{i+1} = -\tilde{\mathbf{A}}'^{-1} \cdot \boldsymbol{f}(\tilde{\boldsymbol{x}}_i) + \tilde{\boldsymbol{x}}_i \equiv \delta\tilde{\boldsymbol{x}}_i + \tilde{\boldsymbol{x}}_i \tag{3.22}$$

where the (transpose of the) z-dimensional vectors

$$\tilde{\boldsymbol{x}}^{\mathrm{T}} = (\rho_1, m_1, \ldots, \rho_\Phi, m_\Phi), \tag{3.23a}$$

$$\boldsymbol{f}^{\mathrm{T}}(\tilde{\boldsymbol{x}}) = (h_1^1, h_2^1, \ldots, h_1^\Phi, h_2^\Phi) \tag{3.23b}$$

and the $z \times z$ matrix $\tilde{\mathbf{A}}'$ replace the $2z \times 2z$ matrix $\mathbf{D}$ which considerably reduces the numerical efforts necessary in solving the original Eq. (3.7) iteratively.

In practice, starting from a suitable solution $\tilde{\boldsymbol{x}}_0^\alpha$ for a given phase $\mathcal{P}^\alpha$ we solve Eq. (3.22) iteratively until $|\boldsymbol{f}(\tilde{\boldsymbol{x}}_{i+1})| \leqslant 10^{-11}$ which requires typically 10^2–10^3 iterations. Under this condition, $\tilde{\boldsymbol{x}}_{i+1}$ is a(n approximate, numerical) solution of the equation

$$\boldsymbol{f}(\tilde{\boldsymbol{x}}) = \mathbf{0}. \tag{3.24}$$

D. Phase equilibria

In general, we are not only interested in solutions of Eq. (3.24) but, more specifically, in those solutions satisfying

$$\omega^{\alpha\beta}(\mu^{\alpha\beta}, T) \equiv \omega^\alpha(\mathcal{P}^\alpha; \mu^{\alpha\beta}, T) = \omega^\beta(\mathcal{P}^\beta; \mu^{\alpha\beta}, T). \tag{3.25}$$

Equation (3.25) defines the chemical potential at coexistence $\mu^{\alpha\beta}$ between phases $\mathcal{P}^\alpha$ and $\mathcal{P}^\beta$ for a given temperature T. To determine $\mu^{\alpha\beta}$ at a slightly different temperature $T' = T + \delta T$ we expand ω in a Taylor series around some chemical potential μ_i, say, that is

$$\begin{aligned} \omega^{\alpha,\beta}(\mu_{i+1}) &= \omega^{\alpha,\beta}(\mu_i) + \left.\frac{\mathrm{d}\omega^{\alpha,\beta}}{\mathrm{d}\mu}\right|_{\mu=\mu_i} (\mu_i - \mu_{i+1}) \\ &\quad + O((\mu_i - \mu_{i+1})^2) \\ &\simeq \omega^{\alpha,\beta}(\mu_i) - \overline{\rho}_i^{\alpha,\beta}(\mu_i - \mu_{i+1}), \quad T' = \text{const} \end{aligned} \tag{3.26}$$

where we dropped all other arguments to ease the notational burden. The far right side of Eq. (3.26) follows from the fact that

$$\begin{aligned} \frac{\mathrm{d}\omega}{\mathrm{d}\mu} &= \sum_{l=1}^{z} \left(\frac{\partial\omega}{\partial\rho_l}\frac{\mathrm{d}\rho_l}{\mathrm{d}\mu} + \frac{\partial\omega}{\partial m_l}\frac{\mathrm{d}m_l}{\mathrm{d}\mu}\right) + \frac{\partial\omega}{\partial\mu} = \frac{\partial\omega}{\partial\mu} \\ &= -\frac{1}{z}\sum_{l=1}^{z}\rho_l = -\overline{\rho}, \end{aligned} \tag{3.27}$$

where Eqs. (2.12) and (B4) have also been employed and $\overline{\rho}$ is the mean density on the *entire* lattice. Assuming Eq. (3.25) to hold for μ_{i+1} we can solve Eq. (3.26) for μ_{i+1} to obtain

$$\mu_{i+1} = \mu_i + \frac{\omega^\beta(\mu_i) - \omega^\alpha(\mu_i)}{\overline{\rho}_i^\beta - \overline{\rho}_i^\alpha}, \tag{3.28}$$

thus providing an iterative scheme to calculate the chemical potential at coexistence. It may be initiated by setting initially $\mu_i = \mu_0^{\alpha\beta}$ at the previous temperature T_0 and calculating $\overline{\rho}_i^{\alpha,\beta}$ from $\tilde{\boldsymbol{x}}^{\alpha,\beta}$ at that temperature.

However, $\tilde{\boldsymbol{x}}^{\alpha,\beta}$ will no longer be solutions of Eq. (3.24) at T' and μ_{i+1}. Hence, we solve Eqs. (3.24) and (3.28) until $|\delta\mu| \equiv \mu_{i+1}^{\alpha\beta} - \mu_i^{\alpha\beta} \lesssim 10^{-11}$. Hence, for a given temperature $\mathcal{P}^\alpha$ and $\mathcal{P}^\beta$ coexist at a chemical potential $\mu^{\alpha\beta} \equiv \mu_{i+1}$. However, the associated $\omega^{\alpha\beta}$ does not necessarily correspond to the *absolute* but may represent only a *relative* minimum of the grand-potential density. If, on the other hand, for any pair α, β, the grand potential density assumes its *global* minimum, $\mathcal{P}^\alpha$ and $\mathcal{P}^\beta$ are *thermodynamically* stable phases at coexistence. The range of temperatures and chemical potentials over which this condition is satisfied defines the coexistence line $\mu_x^{\alpha\beta}(T)$ between $\mathcal{P}^\alpha$ und $\mathcal{P}^\beta$ as the set

$$\mu_x^{\alpha\beta}(T) = \{\mu^{\alpha\beta}, T \,|\, \omega^{\alpha\beta}(\mu^{\alpha\beta}, T) = \min_\gamma \omega^\gamma(\mathcal{P}^\gamma; \mu^{\alpha\beta}, T)\}. \tag{3.29}$$

Moreover, the subsequent discussion will benefit from introducing the notion of a phase diagram as the union of all coexistence lines, that is,

$$\mu_x(T) = \bigcup_{\alpha,\beta} \mu_x^{\alpha\beta}(T). \tag{3.30}$$

IV. RESULTS

A. Fluid phase properties

1. Impact of the system size

In this work we are exclusively concerned with wetting of a *single* solid substrate by a fluid mixture. However, for

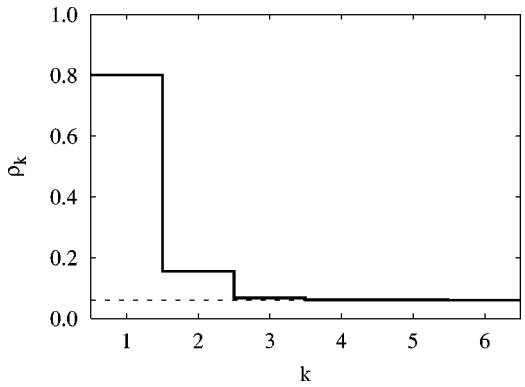

FIG. 1. Local density ρ_k as function of lattice plane k at a critical point $T_c \simeq 0.810$, $\mu_c \simeq -2.464$ at which demixed A- and B-rich phases become indistinguishable. The solid substrate is located at $k=0$. Discontuniuties reflect discrete nature of lattice-gas model. The dashed horizontal line represents bulk density under identical thermodynamic conditions.

purely practical reasons [i.e., in order to minimize the dimension of the vector function $\boldsymbol{f}(\boldsymbol{x})$ in Eq. (3.5)] appropriate boundary conditions have already been introduced. Through the presence of two planar substrates at lattice planes $l=0,z+1$ our system is symmetric with respect to a plane located halfway in between lattice planes $l=\Phi$ and $l=\Phi+1$ (z even) thus permitting us to change variables according to $\boldsymbol{x}\rightarrow\tilde{\boldsymbol{x}}$.

However, for small z the presence of a second substrate will generally cause unwanted confinement effects such as capillary condensation replacing wetting transitions which are the key issue here. To make sure that for the present choice of $z=12$ and moderate fluid-wall attraction ($\epsilon_W=-1.075$) wetting prevails, in Fig. 1 we present the local density ρ_k of an adsorbed film in thermodynamic equilibrium with a bulk gas mixture. The plot in Fig. 1 clearly indicates that the local density of the adsorbed film quickly approaches the density of the homogeneous bulk phase as one departs from the (lower) surface of the solid substrate. The range of distances from the solid substrate over which ρ_k deviates from its constant bulk value is more or less the same regardless of the specific conditions under consideration as we have tested for several points along various coexistence lines. The deviation of the local density from its bulk value remains always short-range even at critical points as the plot in Fig. 1 reveals. This reflects the mean-field approximation for the Hamiltonian. Hence, we conclude that for the present choice of $z=12$ the distance between the solid substrates is sufficiently large so that confinement effects do not interfere with wetting phenomena. In other words, we are *effectively* dealing with phenomena occurring at a *single* solid surface.

TABLE I. Notation to identify phases $\mathcal{P}^{\alpha}$ of asymmetric binary mixtures wetting a selective, chemically homogeneous, planar solid substrate.

α	Nature of phase
G	gas
bF	B-rich film
mF	mixed film
aF	A-rich film
mL	mixed liquid
aL	A-rich liquid

2. Asymmetry of the bulk mixture

The key issue of this work is the combined effects of asymmetry of the mixture (i.e., $\chi_B \neq 1$) and selectivity of the solid substrate (i.e., $\chi_W \neq 1$). To illustrate first the impact of asymmetry we consider as reference the symmetric bulk mixture characterized by $\chi_B=1$. In addition we set $\epsilon_{AB}=-0.5$ and $\epsilon_{AA}=-1.0$ such that the mixture tends to decompose on account of the relatively weak attraction between molecules of unlike species relative to the attraction between like molecules. In Fig. 2(a) we present the phase diagram $\mu_x(T)$ for this special case. It consists of a line of discontinuous phase transitions $\mu_x^{\mathrm{GaL}}(T)$ along which a stable gas phase (G) coexists with a demixed A-rich liquid phase (aL) up to a temperature $T_t \simeq 1.082$ (see Table I). The term "α-rich" therefore refers to the fact that an excess of the α component is present. However, we note in passing that for the symmetric mixture A- and B-rich demixed phases cannot be distinguished in principle. Thus, as far as symmetric mixtures are concerned the term "α-rich" refers only to the fact that an excess of one of the two components is present in the demixed liquid state regardless of which one it is.

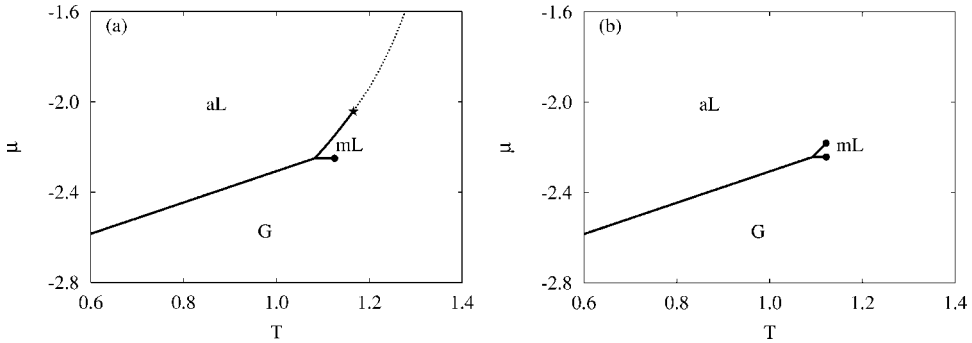

FIG. 2. Phase diagrams $\mu_x(T)$ for bulk mixtures. (a) Symmetric mixture ($\chi_B=1$) where the dotted line represents the λ line starting at a tricritical point (⋆), and (●) represents a critical point. (b) Asymmetric mixture ($\chi_B=0.99$) with two critical points (●). One-phase regions are labeled according to Table I.

TABLE II. Color key to identify coexistence lines $\mu_x^{\alpha\beta}(T)$ along which $\mathcal{P}^\alpha$ and $\mathcal{P}^\beta$ are in thermodynamic equilibrium. The table applies only to the online version of this paper.

$\alpha\beta$	color key
G-aF	
mF-aF	
G-mF	
aF-bF	
mF-bF	
G-bF	

At the temperature $T_t \simeq 1.082$, $\mu_x(T)$ bifurcates into two coexistence lines, namely $\mu_x^{\mathrm{aLmL}}(T)$ ending at a tricritical point $\mu_{\mathrm{tri}} \simeq -2.040$ and $T_{\mathrm{tri}} \simeq 1.166$. At the tricritical point the line of discontinuous phase transitions between mixed and demixed *A*-rich liquid phases changes to a λ line, that is, a line of *continuous* phase transitions between the two phases. The coexistence line $\mu_x^{\mathrm{GmL}}(T)$, on the other hand, terminates at a critical point demarcated by $\mu_c \simeq -2.250$ and $T_c \simeq 1.125$. Hence, the bifurcation of $\mu_x(T)$ at $\mu_t \simeq -2.250$ and $T_t \simeq 1.082$ constitutes a triple point at which a gaseous, mixed liquid and demixed, *A*-rich liquid phase coexist.

A slight asymmetry in the like interactions changes this picture significantly in a number of respects. This can be seen in Fig. 2(b) where we consider the case $\chi_B = 0.99$. First, the triple point is shifted to somewhat higher values $\mu_t \simeq -2.243$ and $T_t \simeq 1.092$. Second, and more importantly, the coexistence line $\mu_x^{\mathrm{aLmL}}(T)$ is shorter compared with the symmetric bulk mixture [see Fig. 2(a)] and ends at a true critical point $\mu_c \simeq -2.182$, $T_c \simeq 1.122$ replacing the tricritical point visible in Fig. 2(a). Hence, the λ line starting at $\mu_{\mathrm{tri}} \simeq -2.040$ and $T_{\mathrm{tri}} \simeq 1.166$ in Fig. 2(a) is absent in Fig. 2(b).

B. Wetting behavior

Henceforth, we fix $\epsilon_{AA} = -1.0$, $\epsilon_{AB} = -0.5$, and $\chi_B = 0.99$, and investigate the impact of χ_W on the wetting behavior of this weakly asymmetric binary mixture. This seems sensible to limit the dimension of the parameter space and because varying χ_B does not alter the generic phase behavior of our model qualitatively. To realize a wall the mixture "desires" to wet preferentially we set $\epsilon_{AW} = -1.075$ so that molecules of component *A* gain potential energy by interacting with the solid substrate rather than with another molecule of either species *A* or *B*.

Before turning to a discussion of our results the reader should, however, realize that a representation of phase diagrams in terms of the mean density of the film $\overline{\rho}$ is inappropriate since this quantity depends on the choice of *z* for wetting films of finite thickness. Likewise a quantitative discussion of the "degree" of miscibility of a particular phase in terms of $\overline{m} \equiv z^{-1} \Sigma_{k=1}^{z} m_k$ is equally unsuitable because it does not take into account the local density of the wetting film such that absolute values of $\overline{m}$ can be quite misleading. Instead we introduce the excess coverage

$$\Gamma \equiv \sum_{k=1}^{\Phi} (\rho_k - \rho_{\mathrm{bulk}}) = \sum_{k=1}^{\Phi} (\rho_k - \rho_\Phi), \tag{4.1}$$

where the far right side follows because for our present choice of parameters $\lim_{k \to \Phi} \rho_k = \rho_{\mathrm{bulk}}$ where ρ_{bulk} is the density of the bulk phase for a given μ and *T*. The excess coverage is a particularly convenient order parameter because it is frequently measured in parallel experimental studies [33]. In a similar spirit we introduce a density-corrected miscibility parameter through the expression

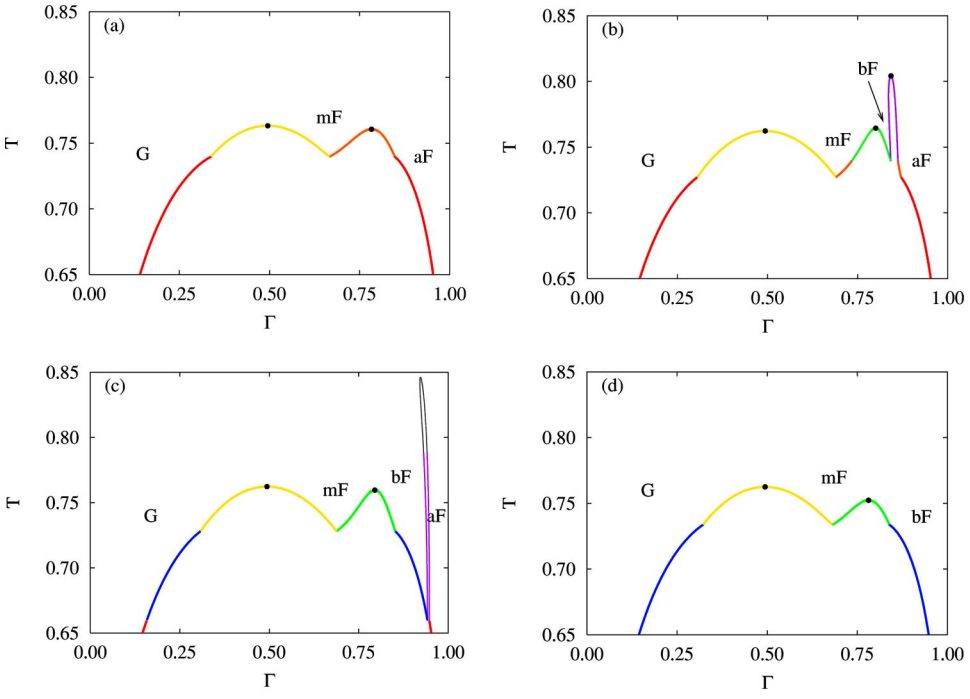

FIG. 3. (Color online) Phase diagrams in the T-Γ representation. (a) $\chi_W = 1.0000$, (b) $\chi_W = 1.0160$, (c) $\chi_W = 1.0175$, and (d) $\chi_W = 1.0250$. See Table II for color key.

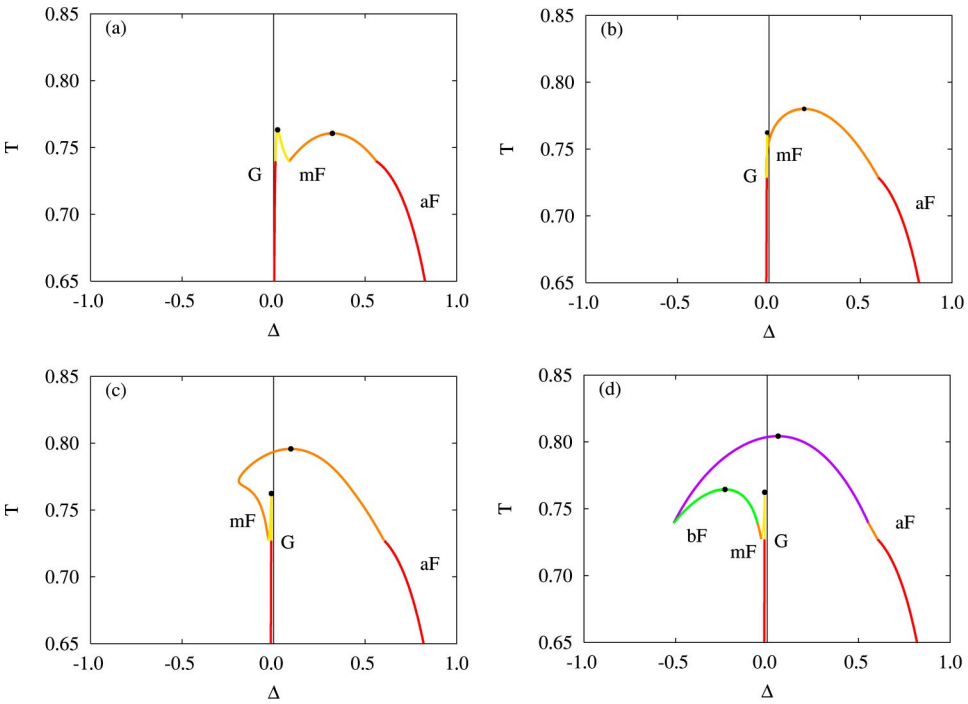

FIG. 4. (Color online). Phase diagrams in the T-Δ representation. (a) $\chi_W=1.000$, (b) $\chi_W=1.0145$, (c) $\chi_W=1.0157$, and (d) $\chi_W=1.0160$. See Table II for color key.

$$\Delta \equiv \frac{1}{\Gamma}\sum_{k=1}^{\Phi} m_k \rho_k \tag{4.2}$$

as a meaningful quantitative measure of the "degree" of miscibility in binary-mixture films.

Since the excess coverage Γ is perhaps the more familiar of the two order parameters we begin by discussing its dependence on χ_W (see Fig. 3). In Fig. 3(a) we plot T as a function of Γ for an asymmetric binary mixture wetting a nonselective wall ($\chi_B=1.000$) which we take as a reference system. The plot shows that for sufficiently low temperatures $T\lesssim 0.740$ a gaseous mixture at low excess coverage $0\lesssim\Gamma\lesssim 0.340$ coexists with an A-rich film at high excess coverage $0.846\lesssim\Gamma\lesssim 1.0$. As T increases further eventually a triple point exists at $T_t\simeq 0.740$ at which a gaseous film coexists simultaneously with a mixed one at intermediate excess coverages and with an A-rich one at high excess coverages. For even higher temperatures the gaseous film coexists with a mixed film whereas mixed films coexist separately with demixed films until the respective critical temperatures at $T_c^{\mathrm{GmF}}\simeq 0.763$ and $T_c^{\mathrm{mFaF}}\simeq 0.761$ are reached.

The nature of the phases cannot be determined solely on the basis of the plot in Fig. 3(a). However, the parallel plot in Fig. 4(a) permits one to identify the specific wetting films without ambiguity. It reveals that the gaseous film is characterized by $\Delta\approx 0$ regardless of T as one would expect. In other words, the gaseous film is nearly perfectly mixed unlike the coexisting A-rich film for which $0.558\lesssim\Delta\lesssim 1.0$ depending on T. That is, the asymmetry of the (bulk) mixture favoring the formation of A-rich mixtures prevails even in the immediate vicinity of the solid substrate. Figure 4(a) also shows that the mixed films coexisting with either gas or A-rich demixed films is characterized by $\Delta\gtrsim 0$, so that it too has a tendency towards formation of A-rich films despite their larger degree of miscibility (i.e., the smaller value of Δ) compared with the latter.

If the substrate is selective this picture becomes considerably richer. This is apparent from the plot in Fig. 3(b) where we plot T as a function of Γ for $\chi_W=1.0160$. For this value of χ_W molecules of species B are preferentially adsorbed by the substrate such that the fluid–substrate interaction counterbalances to some extent the asymmetry of the mixture. As a consequence the plot in Fig. 3(b) is morphologically distinct from the one displayed in Fig. 3(a) in that now a thermodynamically stable, demixed B-rich film coexists with both a mixed B-rich film and a demixed A-rich film. As χ_W increases further the one-phase region of the (demixed) B-rich film widens and tends to gradually replace the (demixed) A-rich film as a comparison between Figs. 3(b) and 3(c) indicates. This causes the critical point of the A- and B-rich demixed films to be located *above* the coexistence line $\mu_x^{\mathrm{GaL}}(T)$ in the bulk so that the A-rich wetting film becomes metastable over a regime indicated by the gray line in Fig. 3(c). Eventually, at $\chi_W=1.025$, the B-rich demixed phase completely replaces the demixed A-rich one favored by the asymmetry of the binary mixture $\chi_B=0.99$ in the bulk. Thus, for a sufficiently large selectivity the substrate is capable of inducing a decomposition of the adsorbed film that is not favored by the asymmetry of the mixture, that is a B-rich phase is not visible in the bulk phase diagram shown in Fig. 2(b), as one would expect intuitively for our present choice of values for χ_B, ϵ_{AA}, and ϵ_{AB}.

The mechanism through which the B-rich demixed film appears as χ_W increases is revealed in greater detail through plots of T versus Δ in Figs. 4 which show that the critical point at which mixed and demixed A-rich films become indistinguishable increases in temperature but shifts to lower Δ

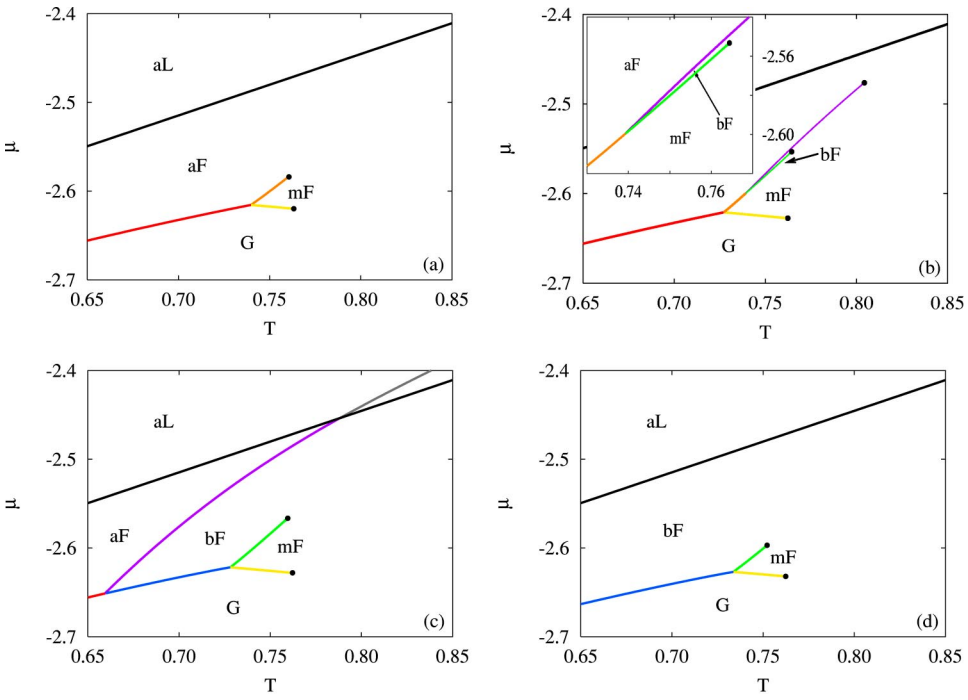

FIG. 5. (Color online) Phase diagrams in the μ-T representation and for χ_W as in Fig. 3. Inset in (b) is an enhancement to emphasize $\mu_x^{\mathrm{mFbF}}(T)$ (see the text). The solid black line represents the coexistence curve $\mu_x^{\mathrm{GaL}}(T)$ in the bulk. See Table II for color key.

[see Figs. 4(a), 4(b), and 4(c)]. This indicates that with increasing χ_W the mixed film contains a larger mole fraction of component *B*. For sufficiently large χ_W component *B* begins to dominate the composition of the mixed film over a certain range of temperatures [see Fig. 4(c)]. With increasing T this effect becomes more pronounced at first over a range $0.728 \lesssim T \lesssim T_{\mathrm{inv}}$ where the ''inversion'' temperature is defined as

$$\left.\frac{\mathrm{d}\Delta}{\mathrm{d}T}\right|_{T=T_{\mathrm{inv}}} = 0. \tag{4.3}$$

For $T > T_{\mathrm{inv}}$ the composition of the mixed film changes towards a larger mole fraction of species *A* all the way up to the critical temperature $T_c \simeq 0.796$ as the plot in Fig. 4(c) clearly shows.

Eventually, for sufficiently large $\chi_W = 1.0160$ the plot in Fig. 4(d) reveals that a *B*-rich, demixed film has entered the picture. Hence, the coexistence between a mixed and demixed, *A*-rich film is replaced by coexistence between *A*- and *B*-rich demixed films for temperatures somewhat below the critical point demarcated by $T_c = 0.804$ and $\Delta = 0.058$. Just prior to reaching this critical point, however, the composition of the demixed film changes to the extent that it again becomes (weakly) *A* rich. In addition, two other critical points between a mixed and a demixed, *B*-rich film ($T_c = 0.764$ and $\Delta = -0.230$) and between a mixed *B*-rich and a gaseous film are present ($T_c = 0.762$ and $\Delta = -0.013$).

The dependence of mixture properties on the attraction strength of the solid substrate is illustrated in greater detail by the phase diagrams $\mu_x(T)$ plotted in Fig. 5. Taking Fig. 5(a) as a reference we note by comparing it with the plot in Fig. 5(b) that two new coexistence lines namely, $\mu_x^{\mathrm{aFbF}}(T)$ and $\mu_x^{\mathrm{bFmF}}(T)$ arise. As one can see from the inset in Fig. 5(b) these two coexistence lines have different slopes such that a triple point between a mixed film and demixed *A*- and *B*-rich films occurs ($T_t \simeq 0.739$ and $\mu_t \simeq -2.600$). Further increase of χ_W causes this new triple point to shift in the direction of the already existing one at which a gaseous, mixed and demixed *A*-rich film coexist [see Figs. 5(a) and 5(b)]. Eventually, the two triple points coincide thereby giving rise to a quadruple point at which all four phases (i.e., gaseous, mixed, and demixed, *A*- and *B*-rich films) are in coexistence. Increasing χ_W even further beyond this point causes the one-phase region of the demixed, *B*-rich film to widen as the plot in Fig. 5(c) illustrates. Since the one-phase region of the *A*-rich demixed film is then completely surrounded by other coexistence lines and the ordinate $T = 0$ thermodynamically stable demixed *A*-rich films are formed exclusively through discontinuous phase transitions. Widening of the one-phase region of demixed, *B*-rich films continues until the one-phase region of the demixed, *A*-rich films has been entirely removed from the phase diagram [see Fig. 5(d)].

V. SUMMARY AND CONCLUSIONS

In this work we focus on the wetting characteristics of an asymmetric binary mixture near a selective, planar, and chemically homogeneous substrate. Model parameters are tuned such that in the bulk the mixture tends to phase separate where the asymmetry (i.e., difference in attraction strength between *A*-*A* and *B*-*B* interactions) is chosen such that in the demixed liquid state the formation of *A*-rich phases is favored. We employ a lattice model and assume a mean–field representation of the intrinsic free energy (functional). Even though this may seem an oversimplification of ''real'' fluid mixtures at first glance, it is noteworthy that results obtained for such a model can be brought into semiquantitative agreement with recent experimental data pro-

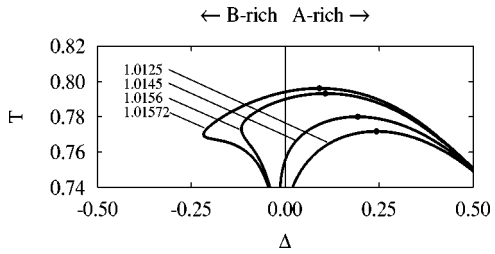

FIG. 6. Plots of T vs Δ for coexistence between demixed A-rich and mixed films of various compositions for several values of χ_W indicated in the figure. (●) demarcates the critical points.

vided model parameters are chosen sensibly [33].

In the present work it turns out that even very slight deviations of χ_B from the symmetric case $\chi_B=1$ suffice to completely suppress the formation of demixed B-rich liquid phases in the bulk. This overall picture does not change qualitatively for all $\chi_B<1$. Hence, the special case of a symmetric mixture ($\chi_B=1$) considered previously by us [29] and others [23–26] appears to have a somewhat ''singular'' character.

Taking the present asymmetric mixture as a reference it seems most interesting to choose the selectivity of the solid substrate such that the fluid-substrate interactions compete with the fluid-fluid ones in the sense that the substrate energetically prefers molecules of species B whereas in the bulk formation of A-A pairs is energetically favored.

Our main results can then be summarized as follows. For $\chi_W=1.0$ (i.e., for a nonselective solid substrate) a demixed A-rich film coexists with a mixed one in which the mole fraction of species A exceeds that of species B. That is, even though the film appears to be more or less mixed indicated by a lower value of Δ, it still preserves a tendency towards forming A-rich phases. This simply reflects the physical nature of our reference (bulk) mixture. As χ_W increases, the composition of the mixed film changes until eventually the concentration of molecules of species B dominates.

However, the composition of the mixed B-rich films exhibits a nonmonotonic temperature dependence. This is illustrated by the plot in Fig. 6 which shows that beyond a certain threshold $\chi_W \gtrsim 1.0145$ an inversion temperature exist for the composition of the mixed B-rich film [see Eq. (4.3)]. For $T \leqslant T_{\mathrm{inv}}$ the concentration of B molecules in the mixed film coexisting with a demixed A-rich film increases steadily. This temperature dependence is inverted for $T \geqslant T_{\mathrm{inv}}$. Now, the concentration of molecules of species B decreases with T until eventually the concentration of molecules of species A in the mixed film exceeds that of molecules of species B. The inversion temperature decreases slightly with increasing χ_W, as plots in Fig. 6 show.

Beyond a certain threshold $\chi_W \gtrsim 1.01574$ a stable demixed, B-rich film appears, coexisting separately with a mixed B-rich one and a demixed A-rich one. By varying χ_W appropriately all four phases (i.e., gaseous, mixed B rich, and demixed A- and B-rich films) may coexist at a quadruple point. Thus, by fine tuning the fluid-substrate attraction one may change the physical nature of adsorbed wetting films in rather spectacular ways. For intermediate selectivities one may support a tendency towards mixing a binary fluid such that initially A-rich films eventually become B rich. The concentration of component B in these films is maximum at the inversion temperature T_{inv}. For sufficiently high selectivities the substrate may induce demixing of these B-rich wetting films to the extent that demixed A-rich films are completely absent.

These phenomena should in principle be observable in parallel experiments where the solid surface is modified chemically in a controlled and quantitative manner. As expected this chemical modification alters the fluid-substrate attraction [33]. However, experimentally it is generally quite difficult to modify a solid surface such that the interaction with a given fluid (mixture) can be varied nearly on a continuous scale. Nevertheless, we anticipate our results to be useful in the interpretation of experimental investigations of wetting of chemically modified substrates by fluid mixtures [34–36]. In these latter works x-ray reflectivity and diffuse scattering under grazing angles are employed to investigate the wetting behavior of binary organic mixtures wetting silica and fused-silica surfaces. In Ref. [35], for example, the authors focus on liquid-gas interfaces and find a significant change in composition of the wetting film as the bulk coexistence line is approached. Similar effects are observed here. For instance, approaching in Fig. 5(c) the bulk coexistence line from below along the isotherm $T=0.75$ one realizes that an originally mixed film undergoes a transition to a demixed B-rich film which is eventually transformed discontinuously into a demixed A-rich film sufficiently close to the bulk coexistence line.

Another important question the present work does not address is related to phase behavior of asymmetric mixtures if they are confined to spaces of nanoscopic dimension(s). Again the interplay between asymmetry of the fluid–fluid interactions and selectivity of the solid substrate is expected to induce a complex phase behavior where the degree of confinement (e.g., the size of nanoscopic pores) will become an additional parameter that determines the phase behavior to a large extent. The behavior of fluid mixtures in confined spaces is important in a variety of contexts ranging from, say, purification of gas mixtures [37] to catalysis [38]. A study focussing on asymmetric binary mixtures under nanoscopic confinement by selective walls is presently under way [39].

ACKNOWLEDGMENT

We are grateful to the Sonderforschungsbereich 448 ''Mesoskopisch strukturierte Verbundsysteme'' for financial support.

APPENDIX A: DERIVATION OF THE MEAN-FIELD HAMILTONIAN

As was shown in Ref. [29] one can work out expressions for the number N_{AA} (N_{BB}) of A-A(B-B) pairs, that is directly connected sites both of which are occupied by a molecule of species $A(B)$. Likewise, expressions for $N_{AB}(\mathbf{s})$ and the total number of molecules of species A and B at the solid substrate, $N_{AW}(\mathbf{s})$ and $N_{BW}(\mathbf{s})$ have been worked out in Ref.

[29]. The resulting expressions presented in Eqs. (2.4)–(2.7) of Ref. [29] contain terms that can be cast as

$$\sum_{k,l} s_{k,l}s_{k,l\pm1}=\sum_{k,l} s_{k,l}\rho_{l\pm1}m_{l\pm1}=n\sum_{l} \rho_l\rho_{l\pm1}m_lm_{l\pm1}, \tag{A1a}$$

$$\sum_{k,l} s_{k,l}s^2_{k,l\pm1}=\sum_{k,l} s_{k,l}\rho_{l\pm1}=n\sum_{l} \rho_l\rho_{l\pm1}m_l, \tag{A1b}$$

$$\sum_{k,l} s^2_{k,l}s^2_{k,l\pm1}=\sum_{k,l} s^2_{k,l}\rho_{l\pm1}=n\sum_{l} \rho_l\rho_{l\pm1}, \tag{A1c}$$

$$\sum_{k,l} s^2_{k,l}s_{k,l\pm1}=\sum_{k,l} s^2_{k,l}\rho_{l\pm1}m_{l\pm1}=n\sum_{l} \rho_l\rho_{l\pm1}m_{l\pm1} \tag{A1d}$$

at the mean-field level. In addition,

$$\sum_{k,l} s_{k,l}\sum_{m=1}^{\mathrm{NN}(k)} s_{m,l}=4\sum_{k,l} s_{k,l}\rho_lm_l=4n\sum_{l} \rho_l^2m_l^2, \tag{A2a}$$

$$\sum_{k,l} s_{k,l}\sum_{m=1}^{\mathrm{NN}(k)} s^2_{m,l}=4\sum_{k,l} s_{k,l}\rho_l=4n\sum_{l} \rho_l^2m_l, \tag{A2b}$$

$$\sum_{k,l} s^2_{k,l}\sum_{m=1}^{\mathrm{NN}(k)} s^2_{m,l}=4\sum_{k,l} s_{k,l}\rho_l=4n\sum_{l} \rho_l^2, \tag{A2c}$$

$$\sum_{k,l} s^2_{k,l}\sum_{m=1}^{\mathrm{NN}(k)} s_{m,l}=4\sum_{k,l} s^2_{k,l}\rho_lm_l=4n\sum_{l} \rho_l^2m_l \tag{A2d}$$

arise where the summation over the four nearest neighbors (k) of lattice site k can be carried out explicitly if Eqs. (2.6) and (2.7) are invoked. Finally,

$$\sum_{k} s_{k,l}=n\rho_lm_l, \tag{A3a}$$

$$\sum_{k} s^2_{k,l}=n\rho_l \tag{A3b}$$

may be employed in Eqs. (2.4) and (2.5) of Ref. [29] to replace the sum over sites in lattice planes $l=1,z$.

Hence, Eqs. (A1) as well as (A3) permit us to write down the mean-field expressions

$$N_{AA}(\boldsymbol{\rho},\boldsymbol{m})=\frac{n}{8}\sum_{l=1}^{z}[\rho_l\rho_{l+1}(m_l+1)(m_{l+1}+1)+\rho_l\rho_{l-1}(m_l+1)(m_{l-1}+1)+4\rho_l^2(m_l+1)^2], \tag{A4a}$$

$$N_{BB}(\boldsymbol{\rho},\boldsymbol{m})=\frac{n}{8}\sum_{l=1}^{z}[\rho_l\rho_{l+1}(m_l-1)(m_{l+1}-1)+\rho_l\rho_{l-1}(m_l-1)(m_{l-1}-1)+4\rho_l^2(m_l-1)^2], \tag{A4b}$$

$$N_{AB}(\boldsymbol{\rho},\boldsymbol{m})=\frac{n}{4}[\rho_l\rho_{l+1}(1-m_lm_{l+1})+\rho_l\rho_{l-1}(1-m_lm_{l-1})+4\rho_l^2(1-m_lm_l)], \tag{A4c}$$

$$N_{AW}(\boldsymbol{\rho},\boldsymbol{m})=\frac{n}{2}[\rho_1(1+m_1)+\rho_z(1+m_z)], \tag{A4d}$$

$$N_{BW}(\boldsymbol{\rho},\boldsymbol{m})=\frac{n}{2}[\rho_1(1-m_1)+\rho_z(1-m_z)], \tag{A4e}$$

which follow after somewhat tedious but straightforward algebraic manipulations.

Replacing now in Eq. (2.2), $N_{ij}(\mathbf{s})$ and $N_{iW}(\mathbf{s})(i,j=A,B)$ by their mean-field counterparts given in Eqs. (A4) eventually yields

$$\begin{aligned}\mathcal{H}_{\mathrm{mf}}(\boldsymbol{\rho},\boldsymbol{m})=&\frac{\epsilon n}{8}\sum_{l=1}^{z}[\rho_l\rho_{l+1}(m_l+1)(m_{l+1}+1)+\rho_l\rho_{l-1}(m_l+1)(m_{l-1}+1)+4\rho_l\rho_l(m_l+1)^2]\\&+\frac{\epsilon\chi_bn}{8}\sum_{l=1}^{z}[\rho_l\rho_{l+1}(m_l-1)(m_{l+1}-1)+\rho_l\rho_{l-1}(m_l-1)(m_{l-1}-1)+4\rho_l\rho_l(m_l-1)^2]+\frac{\epsilon_{AB}n}{4}\\&\times\sum_{l=1}^{z}\Bigg[\rho_l\rho_{l+1}(1-m_lm_{l+1})+\rho_l\rho_{l-1}(1-m_lm_{l-1})+4\rho_l\rho_l(1-m_lm_l)+\frac{\epsilon_{AW}n}{2}[\rho_1(1+m_1)+\rho_z(1+m_z)]\\&+\frac{\epsilon_{AW}\chi_wn}{2}[\rho_1(1-m_1)+\rho_z(1-m_z)]-n\sum_{l=1}^{z}\rho_l\mu\end{aligned} \tag{A5}$$

as the mean-field analog of $\mathcal{H}$ given in Eq. (2.2). In Eq. (A5) the first two sums account for the interaction between a pair of

molecules of species A and B, respectively. Likewise, the third sum represents the contribution of A-B attractions to the mean-field Hamiltonian. The next two terms represent the interaction between a molecule of species A and B with the solid substrate and the last term couples the system to an (infinitely large) external reservoir of matter. Moreover, it is easy to verify from Eq. (A5) that in the limit of a symmetric binary mixture ($\chi_b=1$) and a nonselective solid substrate ($\chi_w=1$) we recover the expression given in Eq. (2.10) of Ref. [29].

APPENDIX B: DERIVATION OF EQS. (2.12)

To derive Eqs. (2.12) we depart from Eq. (2.10) which may be written more explicitly as

$$\Theta(\boldsymbol{n},\boldsymbol{m})=\prod_{l=1}^{z}\frac{n^n}{(n-n_l)^{n-n_l}\left(n_l\frac{1+m_l}{2}\right)^{n_l(1+m_l)/2}\left(n_l\frac{1-m_l}{2}\right)^{n_l(1-m_l)/2}}, \tag{B1}$$

in the limit $n,\{n_l\}\to\infty$ using Stirling's approximation [29]. Using [see Eqs. (2.6) and (2.7)]

$$\rho_l^A=\rho_l\left(\frac{1+m_l}{2}\right), \tag{B2a}$$

$$\rho_l^B=\rho_l\left(\frac{1-m_l}{2}\right), \tag{B2b}$$

so that Eq. (B1) may be recast as

$$\ln\Theta(\boldsymbol{\rho},\boldsymbol{m})=-n\sum_{l=1}^{z}\left\{\rho_l\ln\rho_l+(1-\rho_l)\ln(1-\rho_l)-\rho_l\ln 2+\frac{\rho_l}{2}[(1+m_l)\ln(1+m_l)+(1-m_l)\ln(1-m_l)]\right\}. \tag{B3}$$

Hence, together with Eqs. (2.11) and (A5), Eq. (B3) yields

$$\begin{aligned}\omega(\boldsymbol{\rho},\boldsymbol{m};T,\mu)=&\frac{k_BT}{z}\sum_{l=1}^{z}[\rho_l\ln\rho_l+(1-\rho_l)\ln(1-\rho_l)-\rho_l\ln 2]+\frac{k_BT}{2z}\sum_{l=1}^{z}\rho_l[(1+m_l)\ln(1+m_l)+(1-m_l)\ln(1-m_l)]\\&+\frac{\epsilon}{8z}\sum_{l=1}^{z}[\rho_l\rho_{l+1}(m_l+1)(m_{l+1}+1)+\rho_l\rho_{l-1}(m_l+1)(m_{l-1}+1)+4\rho_l\rho_l(m_l+1)^2]\\&+\frac{\epsilon\chi_b}{8z}\sum_{l=1}^{z}[\rho_l\rho_{l+1}(m_l-1)(m_{l+1}-1)+\rho_l\rho_{l-1}(m_l-1)(m_{l-1}-1)+4\rho_l\rho_l(m_l-1)^2]\\&+\frac{\epsilon_{AB}}{4z}\sum_{l=1}^{z}[\rho_l\rho_{l+1}(1-m_lm_{l+1})+\rho_l\rho_{l-1}(1-m_lm_{l-1})+4\rho_l\rho_l(1-m_lm_l)]\\&+\frac{\epsilon_{AW}}{2z}[\rho_1(m_1+1)+\rho_z(m_z+1)]-\frac{\epsilon_{AW}\chi_w}{2z}[\rho_1(m_1-1)+\rho_z(m_z-1)]-\frac{1}{z}\sum_{l=1}^{z}\rho_l\mu.\end{aligned} \tag{B4}$$

Differentiating Eq. (B4) according to Eqs. (2.12) we find

$$\begin{aligned}h_1^k=&-\overline{\mu}+\beta^{-1}\left[\ln\frac{\rho_k}{1-\rho_k}+\frac{1}{2}\{(1+m_k)\ln(1+m_k)+(1-m_k)\ln(1-m_k)\}\right]+\frac{\epsilon}{4}(m_k+1)[\rho_{k+1}(m_{k+1}+1)+\rho_{k-1}(m_{k-1}+1)\\&+4\rho_k(m_k+1)]+\frac{\epsilon\chi_b}{4}(m_k-1)[\rho_{k+1}(m_{k+1}-1)+\rho_{k-1}(m_{k-1}-1)+4\rho_k(m_k-1)]+\frac{\epsilon_{AB}}{2}[\rho_{k+1}(1-m_km_{k+1})\\&+\rho_{k-1}(1-m_km_{k-1})+4\rho_k(1-m_k^2)]+\frac{\epsilon_{AW}}{2}\{\delta_{k1}[(1+m_1)+\chi_w(1-m_1)]+\delta_{kz}[(1+m_z)+\chi_w(1-m_z)]\}\end{aligned} \tag{B5a}$$

$$h_2^k=\frac{\rho_k}{2}\Bigg[\beta^{-1}\ln\frac{1+m_k}{1-m_k}+\frac{\epsilon}{2}[\rho_{k+1}(m_{k+1}+1)+\rho_{k-1}(m_{k-1}+1)+4\rho_k(m_k+1)]$$

$$+\frac{\epsilon\chi_b}{2}[\rho_{k+1}(m_{k+1}-1)+\rho_{k-1}(m_{k-1}-1)+4\rho_k(m_k-1)]$$

$$+\frac{\epsilon_{AB}}{2}[\rho_{k+1}(1-m_km_{k+1})+\rho_{k-1}(1-m_km_{k-1})+4\rho_k(1-m_k^2)]$$

$$+\frac{\epsilon_{AW}}{2}[\delta_{k1}\{m_1(1-\chi_w)+1-\chi_w\}+\delta_{kz}\{m_z(1+\chi_w)+1+\chi_w\}]\Bigg] \tag{B5b}$$

where $\bar{\mu}\equiv\mu-\beta^{-1}\ln 2$ and δ_{ij} is the Kronecker symbol.

[1] P.G. de Gennes, Rev. Mod. Phys. **57**, 827 (1985).
[2] D. E. Sullivan and M. M. Telo da Gama, in *Fluid Interfacial Phenomena*, edited by C. A. Croxton (Wiley, New York, 1986).
[3] S. Dietrich, in *Phase Transitions and Critical Phenomena*, edited by C. Domb and J. L. Lebowitz (Academic Press, London, 1988), Vol. 12.
[4] M. Schick, in *Liquids at Interfaces*, Les Houches Session XLVIII, edited by J. Charvolin, J. F. Joanny, and J. Zinn–Justin (North-Holland, Amsterdam, 1990), p. 415.
[5] D. Bonn and D. Ross, Rep. Prog. Phys. **64**, 1085 (2001).
[6] R. Evans and M. Chan, Phys. World **9**, 48 (1996).
[7] H. Cao, Z.N. Yu, J. Wang, J.O. Tegenfeldt, R.H. Austin, E. Chen, W. Wu, and S.Y. Chou, Appl. Phys. Lett. **81**, 174 (2002).
[8] A.V. Melechko, T.E. McKnight, M.A. Guillorn, V.I. Merkulov, B. Illic, M.J. Doktycz, D.H. Lowndes, and M.L. Simpson, Appl. Phys. Lett. **82**, 976 (2003).
[9] T.C. Kuo, D.M. Cannon, J.J. Tulock, M.A. Shannon, J.V. Sweedler, and P.W. Bohn, Anal. Chem. **75**, 1861 (2003).
[10] J. S. Rowlinson and B. Widom, *Molecular Theory of Capillarity* (Oxford University Press, Oxford, 1982).
[11] J.G. Dash, Phys. Rev. B **15**, 3136 (1976).
[12] J.W. Cahn, J. Chem. Phys. **66**, 3667 (1977).
[13] C. Ebner and W.F. Saam, Phys. Rev. Lett. **38**, 1486 (1977).
[14] W.F. Saam and C. Ebner, Phys. Rev. A **17**, 1768 (1978).
[15] R. Pandit, M. Schick, and M. Wortis, Phys. Rev. B **26**, 5112 (1982).
[16] D. Nicolaides and R. Evans, Phys. Rev. Lett. **63**, 778 (1989).
[17] S. Dietrich and M. Schick, Phys. Rev. B **33**, 4952 (1985).
[18] K. Binder and D. Landau, Phys. Rev. B **37**, 1745 (1988).
[19] R. Lipowsky, Interface Sci. **9**, 105 (2001).
[20] S. Dietrich, in *Proceedings of the NATO–ASI "New Approaches to Old and New Problems in Liquid State Theory,"* edited by C. Caccamo, J. P. Hansen, and G. Stell (Kluwer, Dordrecht, 1999), p. 197.
[21] C. Rascón and A.O. Parry, Nature **407**, 986 (2000).
[22] S. Sacquin, M. Schoen, and A.H. Fuchs, J. Chem. Phys. **118**, 1453 (2003).
[23] F. Schmid and N.B. Wilding, Phys. Rev. E **63**, 031201 (2001).
[24] Y. Fan, J.E. Finn, and P.A. Monson, J. Chem. Phys. **99**, 8238 (1993).
[25] E. Kierlik, M.L. Rosinberg, Y. Fan, and P.A. Monson, J. Chem. Phys. **101**, 10947 (1994).
[26] N.B. Wilding, F. Schmid, and P. Nielaba, Phys. Rev. E **58**, 2201 (1998).
[27] N. Choudhury and S.K. Ghosh, Phys. Rev. E **64**, 021206 (2001).
[28] R. Evans, in *Liquids at Interfaces*, Les Houches Session XLVIII (Ref. [4]), p. 1.
[29] D. Woywod and M. Schoen, Phys. Rev. E **67**, 026122 (2003).
[30] D. Woywod and M. Schoen (unpublished).
[31] D. A. Lavis and G. M. Bell, *Statistical Mechanics of Lattice Models Vol. I. Closed-Form and Exact Solutions* (Springer-Verlag, Berlin, 1989), p. 60.
[32] H. Bock, D. J. Diestler, and M. Schoen, J. Phys.: Condens. Matter **13**, 4697 (2000).
[33] G. Rother, D. Woywod, G. H. Findenegg, and M. Schoen (unpublished).
[34] A. Plech, U. Klemradt, M. Huber, and J. Peisl, Europhys. Lett. **49**, 583 (1999).
[35] A. Plech, U. Klemradt, and J. Peisl, J. Phys.: Condens. Matter **13**, 5563 (2001).
[36] A. Plech, U. Klemrath, M. Aspelmeyer, M. Huber, and J. Peisl, Phys. Rev. E **65**, 061604 (2002).
[37] R. Denoyel and E. Sabio Rey, Langmuir **14**, 7321 (1998).
[38] N. Y. Chen, T. Degan, Jr., and C. M. Smith, *Molecular Transport and Reaction in Zeolites: Design and Application of Shape Selective Catalysts* (Wiley-VCH, New York, 1994).
[39] D. Woywod and M. Schoen (unpublished).